Supporting Information

A Strategy for Exploiting Self-Trapped Excitons in Semiconductor Nanocrystals for White Light Generation

*Timothy G. Mack, Lakshay Jethi, Patanjali Kambhampati**

Department of Chemistry, McGill University, Montreal, Quebec, H3A 0B8, Canada

Corresponding Author:

*pat.kambhampati@mcgill.ca

S1: Details of the Model:

Generating Franck-Condon Factors

Details of the lineshape calculations can be found in our prior publications[1-2], but will be briefly summarized here . Generally, Franck-Condon factors may be calculated from the Huang-Rhys factor (S), associated Laguerre polynomials (L(S)) and integers corresponding to vibrational initial and final states (n and m) using the following equation:

$$F_n^m = \left|\int \psi_m^* \psi_n dQ\right|^2 = e^{-S} S^{n-m} \left(\frac{m!}{n!}\right) \left(L_m^{n-m}(S)\right)^2 \quad (1)$$

Boltzmann prefactors Ω(ω,T) must be multiplied to the probabilities in the above equation.

With the condition that:

$$\sum \Omega(T) F_m^n = 1 \quad (2)$$

For a Huang-Rhys value of 24.5, the following plot may be obtained:

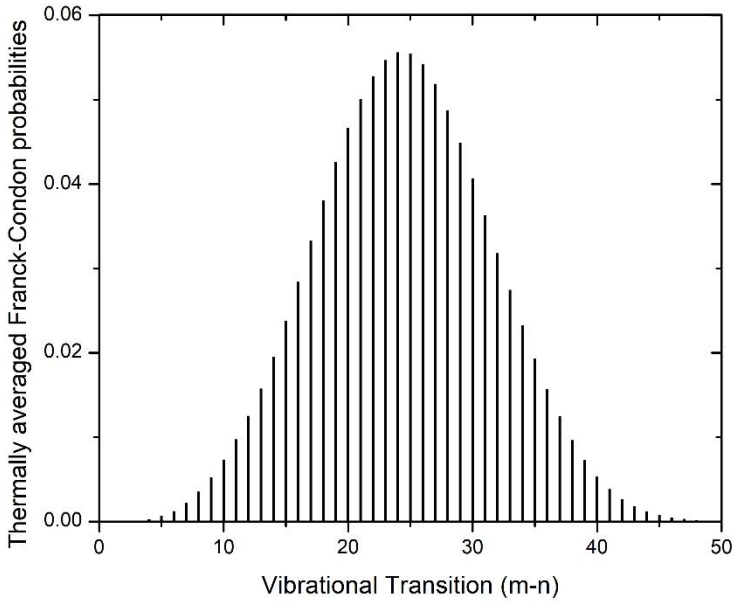

Alternatively, the equivalent lineshape expression below* is perhaps more compactly employed within a programming environment:

$$\sigma(\omega) = |\mu_{eg}|^2 e^{-S(2\overline{n}+1)} \sum_{n=0}^{\infty} \sum_{m=0}^{\infty} \left(\frac{S^{m+n}}{m!n!}\right) (\overline{n}+1)^n \overline{n}^m \delta(\omega - \omega_{eg} - (n-m)\omega_0) \quad (3)$$

where the value of ω_0 is assumed to be the LO phonon mode for bulk CdSe (208 cm^{-1} (25.79 meV)). $\overline{n}$ is the phonon occupation number: $\overline{n} = \left(e^{\left(\frac{\hbar\omega}{kT}\right)} - 1\right)^{-1}$ and ω_{eg} is the excitation frequency.

Each Franck-Condon factor is then broadened by a gaussian lineshape and summed.[3] In this paper an energy mesh of 0.1 meV was chosen. The LO phonon frequency for CdSe is 208 cm^{-1}.

$$\sigma(\omega) = \sum \Omega(T) F_m^n e^{-\frac{1}{2}\left(\frac{E-(m-n)}{\sigma}\right)^2} \quad (4)$$

This process is done for both core and surface, and their respective areas are normalized.

Marcus Jortner theory and steady state approximation:

Following previously published work in our group, the ratio of the core and surface bands can be calculated using Marcus Jortner theory.[1, 4]

The calculation is based on Marcus-Jortner electron transfer theory, in which the medium phonon modes were assumed to be negligible and set to zero (eq. 1).[5]

*http://tdqms.uchicago.edu/sites/tdqms.uchicago.edu/files/uploads/12/12.%20Coupling%20to%20Nuclear%20Motion%2011-20-2014.pdf

$$W = Ae^{-S(2\overline{n}+1)} I_p(2S(\overline{n}(\overline{n}+1)^{\frac{1}{2}}) \left[\frac{(\overline{n}+1)}{\overline{n}}\right]^{\frac{p}{2}} \quad (5)$$

Where $\overline{n}$ is the average phonon occupation number:

$$\overline{n} = \left(e^{\left(\frac{\hbar\omega}{kT}\right)} - 1\right)^{-1} \quad (6)$$

And p is defined as:

$$p = \frac{\Delta G}{\hbar\omega} \quad (7)$$

$I_p(x)$ is the modified Bessel function with imaginary arguments. The variables A is the electronic , which is defined in Jortner's paper. S is the Huang-Rhys parameter.[6]

For the case of figure 4b in the article, the values of 25, 50 and 75 meV of ΔG were used, while all other parameters were held fixed. The Huang Rhys parameter was 20, and the constant $A=10^{13}$. The value of ω is 208 cm^{-1}, which corresponds to the energy of the LO phonon for bulk CdSe.[7] The forward and reverse rates were then calculated through detailed balance approach, in the same manner as previously described in the work of Mooney et al.[4] The forward rate is defined here as W, whereas the reverse rate is $We^{\frac{\Delta G}{k_b T}}$. In this case the radiative lifetime of the core 1S state was set to be 20 ns (τ_r), and the radiative lifetime of the surface state is set to 80 ns (τ_{rS}). which are estimated based on TCSPC measurements. Following the work by Mooney, the following equations were solved using the *fsolve* function MATLAB® 2018a for the values of n_0, n_1, and n_2 which refer to the ground, core 1S and surface state respectively.

$$\frac{dn_0}{dt} = \frac{-n_0}{\tau_0} + \frac{n_1}{\tau_r} + \frac{n_2}{\tau_{rS}} = 0 \quad (8)$$

$$\frac{dn_1}{dt} = \frac{n_0}{\tau_0} - \frac{n_1}{\tau_r} - n_1 W + n_2 W e^{\frac{\Delta G}{k_b T}} = 0 \quad (9)$$

$$\frac{dn_2}{dt} = n_1 W - n_2 W e^{\frac{\Delta G}{k_b T}} - \frac{n_2}{\tau_{rS}} = 0 \quad (10)$$

$$n_0 + n_1 + n_2 = 1 \quad (11)$$

These populations are then related to their emission areas and scaled by their respective lifetimes.

$$A_{1S} = \frac{n_1}{\tau_r} \quad (12)$$

$$A_S = \frac{n_2}{\tau_{rS}} \quad (13)$$

Effect of Lattice contraction:

In this work the effect of lattice contraction is estimated through a linear temperature dependence of 0.3 meV/K, which was estimated by looking at the emission energies of the sample at 300K and 100K. Generally, the temperature dependent lattice contraction can be obtained through the Varshni empirical equation if more accurate values are needed.[8]

S2: CIE Equations:

Emission spectra can be transformed into CIE (International Commission on Illumination / Commission internationale de l'éclairage) coordinates. We summarize these concepts briefly here, but readers should consult relevant colorimetry textbooks for more information.[9] CIE tristimulus values are defined in terms of the integrated response of raw spectral data in units of intensity vs wavelength (in nm) weighted by the three distinct color matching functions (CMF) that span the visible spectrum (380nm -780 nm). There are three CMFs, one for blue, green and red which approximate the physiological responses of the three color types of distinct color cones in the human eye. Usually, the 1931 CMFs are employed, which assume a 2° field of view of the stimulus by a "standard observer", (i.e a human possessing normal color vision), but regardless of the CMFs used, the chromaticity tristimulus values (here in the emissive case) can be calculated as

$$X = \int_{\lambda} L_{e,\Omega,\lambda}(\lambda)\bar{x}(\lambda)d\lambda \tag{14}$$

$$Y = \int_{\lambda} L_{e,\Omega,\lambda}(\lambda)\bar{y}(\lambda)d\lambda \tag{15}$$

$$Z = \int_{\lambda} L_{e,\Omega,\lambda}(\lambda)\bar{z}(\lambda)d\lambda \tag{16}$$

Written in their summation form:

$$X = \sum_{i} \bar{x}_i L_i \Delta\lambda \tag{17}$$

$$Y = \sum_{i} \bar{y}_i L_i \Delta\lambda \tag{18}$$

$$Z = \sum_i \bar{z}_i L_i \Delta\lambda \tag{19}$$

X,Y,Z tristimulus values can then be expressed in terms of normalized CIE chromaticity coordinates (x,y,z):

$$x = \frac{X}{X+Y+Z} \tag{20}$$

$$y = \frac{Y}{X+Y+Z} \tag{21}$$

$$z = \frac{Z}{X+Y+Z} \tag{22}$$

$$x + y + z = 1 \tag{23}$$

Since z can be calculated if x and y are known (equation 23), usually CIE coordinates are reported in terms of (x,y) coordinates, and these coordinates are plotted on the x-y projection which corresponds to the plane of the CIE color space chromaticity diagram as shown below.

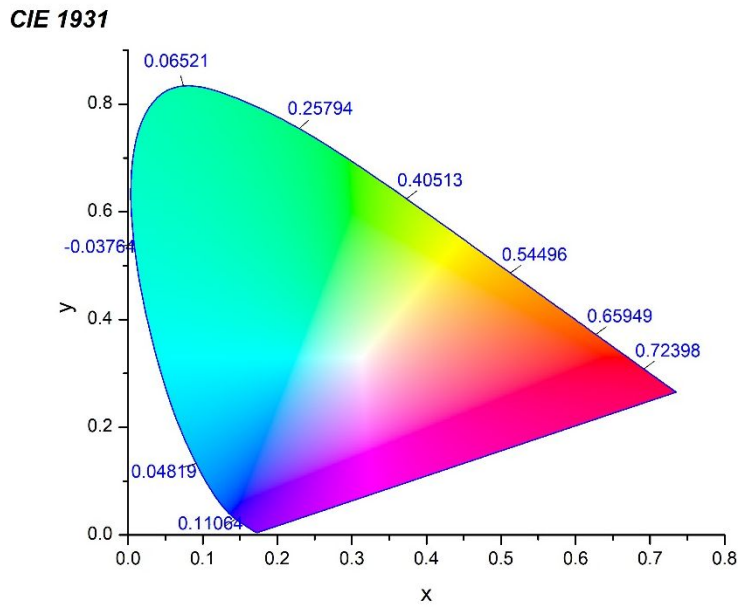

1931 CIE color space Chromaticity diagram,

https://www.originlab.com/fileexchange/details.aspx?fid=168

S3. The 1931 CMFs.

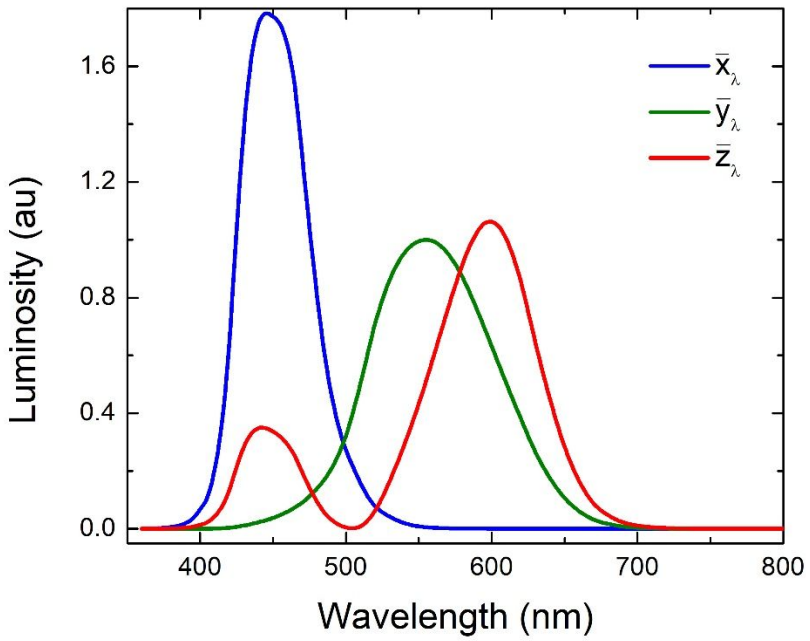

Figure S1: Plot of the 1931 colour matching functions (CMFs).

The CIE chromaticity (x,y) coordinates in this paper are obtained through the use of equations 14-23. Since the 1931 CMFs are spaced by 1 nm increments, experimental photoluminescence data was also collected in 1 nm intervals. For simulated data that had a much finer wavelength resolution, linear interpolation of the CMFs was employed.

S4. Comparison of emission of molecular dye and theoretical 1 nm line source and their CIE (x,y) coordinates

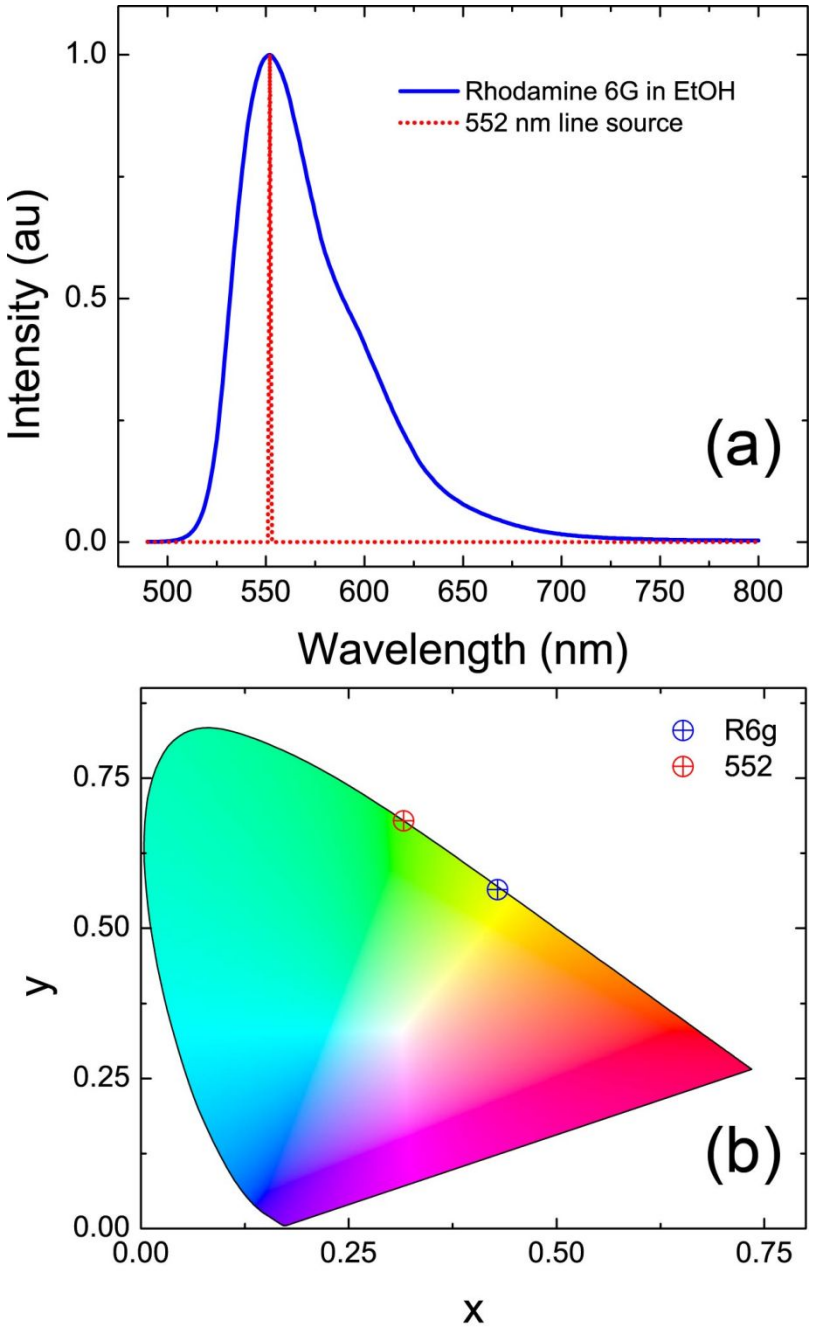

Figure S2: Illustration of conversion from photoluminescence spectra (Panel **(a)**) to (x,y) chromaticity coordinates in the 1931 CIE colour space (Panel **(b))** of a 1 nm line source and of a typical molecular dye (Rhodamine 6 G). A theoretical line source of 1 nm spectra linewidth would lie on the boundary of the chromaticity diagram, by contrast an asymmetric emission of a molecular dye with approximately 30 nm linewidth is slightly off the boundary layer.

Figure S2 illustrates a typical example of a line source and a molecular dye (Rhodamine 6 G) from which to understand the process of conversion from photoluminescence spectra to (x,y) chromaticity coordinates in the 1931 CIE colour space. Transformations of this nature are commonly done and described elsewhere, and well as in the Supporting Information.[refs] A theoretical line source of 1 nm spectra linewidth would lie on the boundary of the chromaticity diagram, by contrast an asymmetric emission of a molecular dye with approximately 30 nm linewidth is slightly closer to the center of the CIE plane. The importance is to note that spectral information cannot be retrieved from chromaticity coordinates. However, chromaticity coordinates provide a simple way compare the spectral output which may be useful for simulating the output of emissive devices as a function of temperature.

S5. Looking at impact of background correction upon calculated CIE coordinates

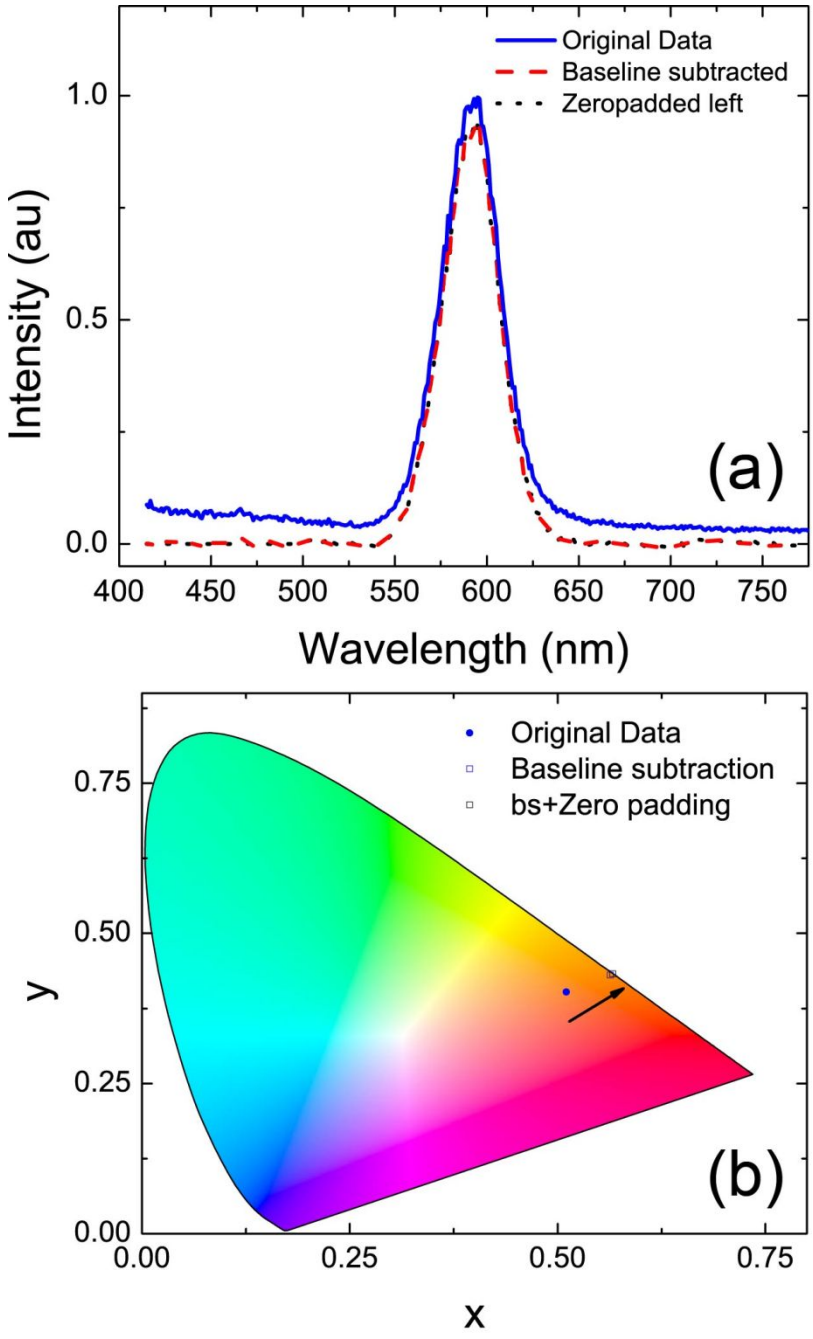

Figure S3: The effect of baseline scatter on the resulting CIE coordinates is illustrated. Panel **(a)** shows the photoluminescence spectra of typical 3.2 nm CdSe NCs embedded in a polystyrene matrix. Panel **(b)** shows the change in CIE coordinates as a function of the the Showing Scattering contribution to the CIE coordinate for low PLQY samples.

Figure S3 shows the importance of addressing potential baseline scatter issues which may be present in NC samples in semiconductor films. We show that a general conversion of the photoluminescence data to CIE coordinates will not necessarily result in the "correct" CIE coordinates if baseline corrections are not conducted. Panel **(a)** shows the corrected and uncorrected photoluminescence spectra of a typical CdSe NC. Panel **(b)** shows the CIE coordinates before and after baseline subtraction. The uncorrected photoluminescence results in a pair of chromaticity coordinates which is significantly blue shifted in comparison with the narrow emission of the NC which has a chromaticity pair much closer to the edge of the CIE diagram.

S6. Polynomial approximation to Core:Surface fitting as empirical alternative to Marcus Jortner theory

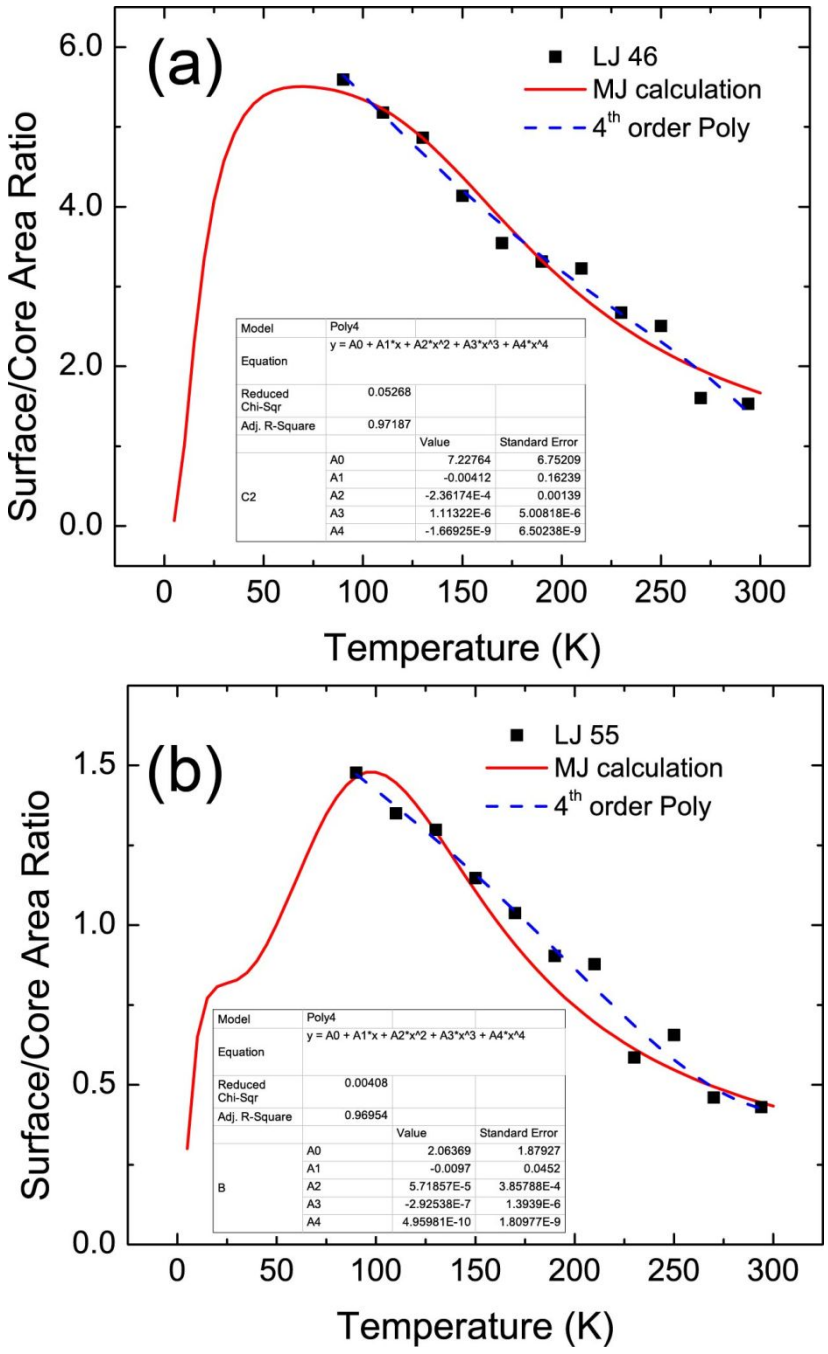

Figure S4: The ratio of photoluminescence intensity of core and surface emissive states between 300K - 90K can be calculated either using semiclassical Marcus-Jortner theory or conveniently approximated through a 4th order polynomial fit. The results are shown for NC sizes of radii 0.89 nm and 1.13 nm in panels **(a)** and **(b)** respectively.

S7. Polynomial fits for size dependence chromaticity calculations

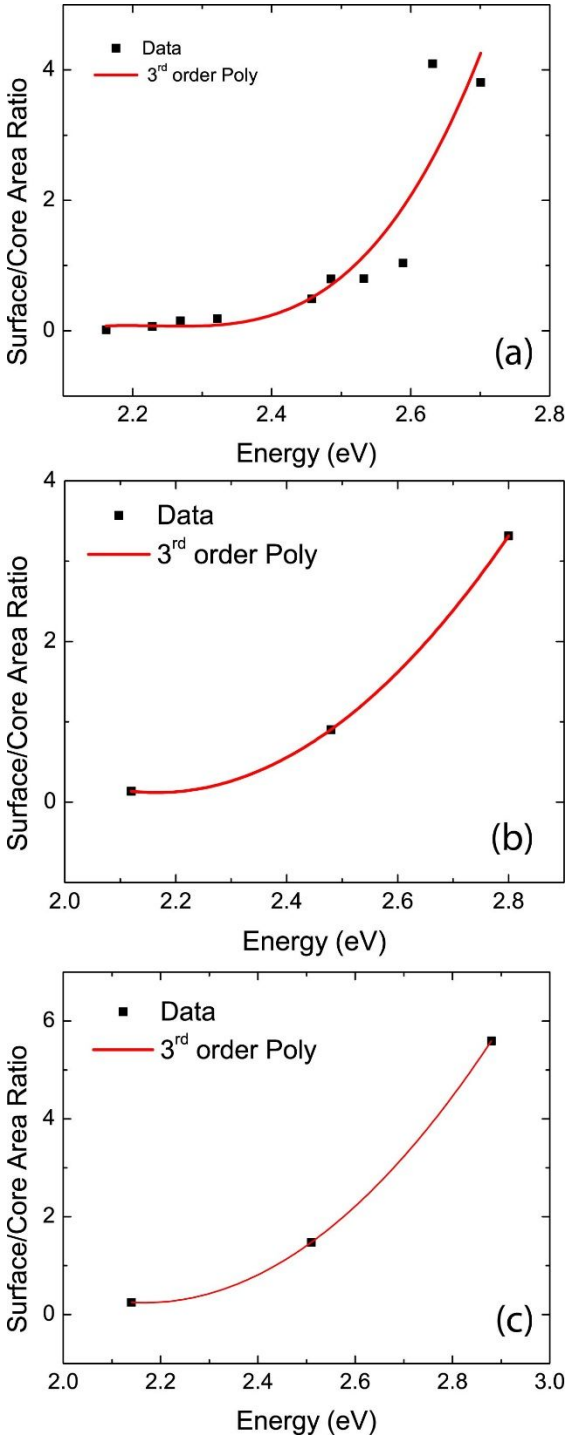

Figure S5: The ratio of photoluminescence intensity of core and surface emissive states for various sizes at 300K **(a)**, 200K **(b)** and 100 K **(c)** are fitted to third order polynomials.

S8. Settings for calculations in figures 5

S=21,

ΔG =20 meV,

Inhomogeneous Linewidth (Gaussian) = 50 meV.

Energies 2.7 eV – 2.1 eV (data point every 20 meV)

S8: Parameters used for calculations in figure 5

Initial Energy 2.55 eV.

Panels a/b

A=1E15, S=21, τ_{core} = 20 ns, $\tau_{surface}$ 80 ns. Linewidth 50 meV

Panels c/d

A=1E15, G=20 meV, τ_{core} = 20 ns, $\tau_{surface}$ 80 ns. Linewidth 50 meV.

S9. Effects on temperature/chromaticity trajectories of other parameters.

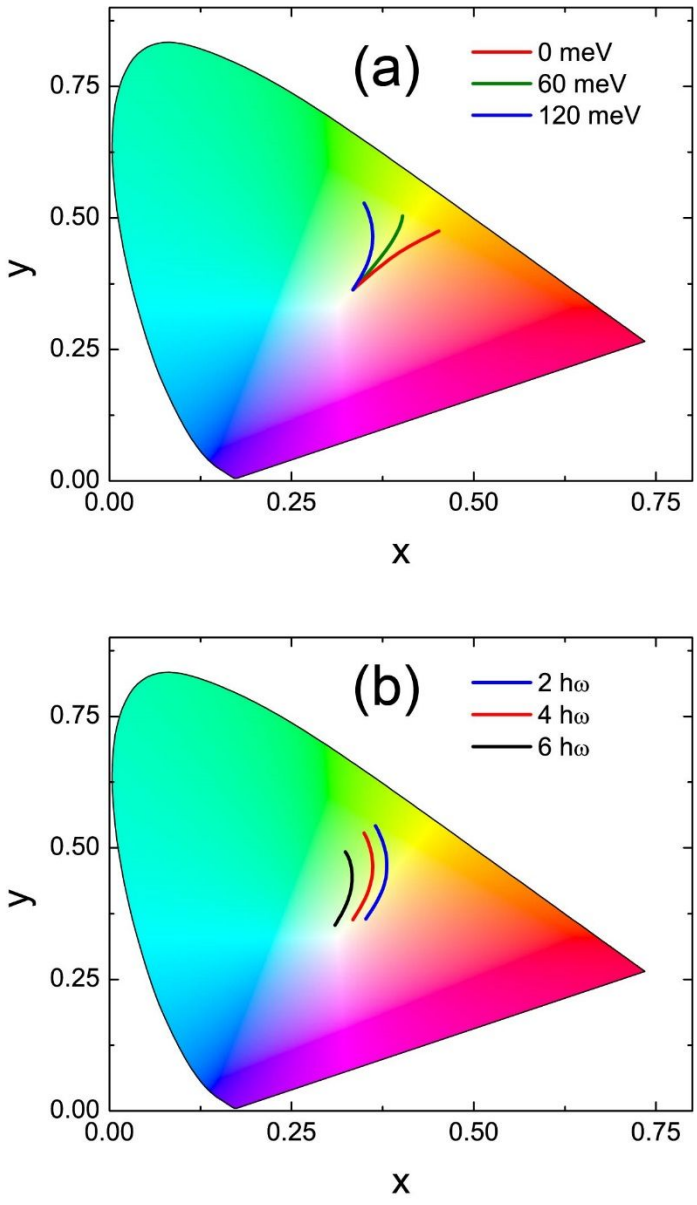

Figure S8: The influence of lattice contraction **(a)** and linewidth **(b)** parameters. The lattice contraction manifests itself as a spectral blueshift, whereas increasing the line broadness of the surface state moves the emission profile to the center of the CIE coordinate space.

Figure S8 shows the effect of varying the lattice contraction energy in meV as a function of temperature linearly from 300 K to 80K. Panel **(b)** shows the effect of varying the linewidth of the surface state in units of ħω.

S10. Temperature dependence simulation (Simulation vs Data)

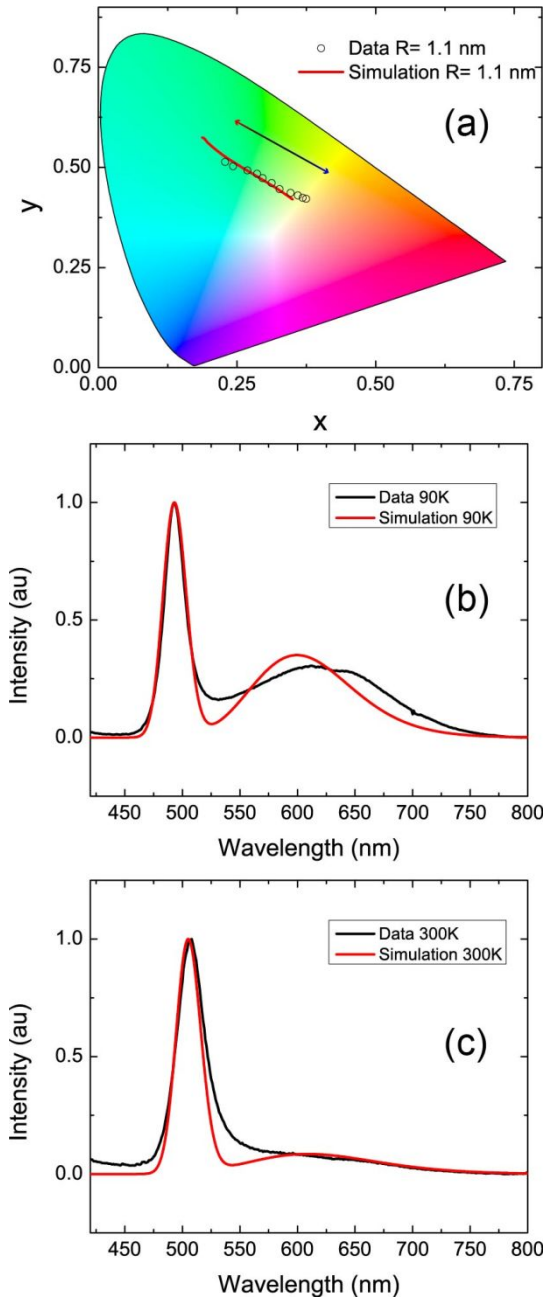

Figure S9 (a) shows CIE temperature trajectory for the 1.1 nm radius sample as function of temperature compared with data. Panels (b) and (c) show the normalized photoluminescence spectra at 90K and 300K respectively, compared with the model simulation. The parameters used in this calculation are as follows. E=2.45 eV, S=18, ω=208 cm^{-1}, ΔG=40 meV, core line

broadening =2hω, (Gaussian), surface line broadening= 4hω (Gaussian). The lattice contraction shift was +60 meV at 90K and was linearly varied for temperatures between 300K and 90K. The core:surface ratio was determined from the 4th order polynomial fit to data in Figure S4, panel (b).

References:

1. Jethi, L.; Mack, T. G.; Kambhampati, P., Extending Semiconductor Nanocrystals from the Quantum Dot Regime to the Molecular Cluster Regime. *The Journal of Physical Chemistry C* **2017,** *121* (46), 26102-26107.
2. Mack, T. G.; Jethi, L.; Kambhampati, P., Temperature Dependence of Emission Line Widths from Semiconductor Nanocrystals Reveals Vibronic Contributions to Line Broadening Processes. *Journal of Physical Chemistry C* **2017,** *121* (51), 28537-28545.
3. de Jong, M.; Seijo, L.; Meijerink, A.; Rabouw, F. T., Resolving the ambiguity in the relation between Stokes shift and Huang–Rhys parameter. *Physical Chemistry Chemical Physics* **2015,** *17* (26), 16959-16969.
4. Mooney, J.; Krause, M. M.; Saari, J. I.; Kambhampati, P., Challenge to the deep-trap model of the surface in semiconductor nanocrystals. *Physical Review B* **2013,** *87* (8), 081201.
5. Jortner, J., Temperature dependent activation energy for electron transfer between biological molecules. *The Journal of Chemical Physics* **1976,** *64* (12), 4860-4867.
6. Huang, K.; Rhys, A., Theory of Light Absorption and Non-Radiative Transitions in F-Centres. *Proceedings of the Royal Society of London. Series A. Mathematical and Physical Sciences* **1950,** *204* (1078), 406-423.
7. Mooney, J.; Saari, J. I.; Myers Kelley, A.; Krause, M. M.; Walsh, B. R.; Kambhampati, P., Control of Phonons in Semiconductor Nanocrystals via Femtosecond Pulse Chirp-Influenced Wavepacket Dynamics and Polarization. *The Journal of Physical Chemistry B* **2013,** *117* (49), 15651-15658.
8. Varshni, Y. P., Temperature dependence of the energy gap in semiconductors. *Physica* **1967,** *34* (1), 149-154.
9. Fairchild, M. D., Color Appearance Models. 3rd ed. ed.; Wiley: Hoboken, 2013.